

Tracking electron-induced carbon contamination and cleaning of Ru surfaces by Auger electron spectroscopy

Aloke Kanjilal,^{a)} Mark Catalano, Sivanandan S. Harilal, and Ahmed Hassanein
*Center for Materials under Extreme Environment, School of Nuclear Engineering, Purdue University,
West Lafayette, Indiana 47907*

Bryan Rice
SEMATECH Inc., Albany, New York 12203

(Received 17 January 2012; accepted 1 May 2012; published 17 May 2012)

Extreme ultraviolet (EUV) radiation induced growth of carbon and oxygen desorption were investigated on a Ru surface by Auger electron spectroscopy (AES) in the presence and absence of additional photoelectrons (PEs) from a focusing Ru mirror. A decrease in EUV reflectivity with carbon growth in the presence of additional PEs has been observed. Conversely, a carbonaceous Ru surface was cleaned in sequential AES, and discussed in terms of secondary electron assisted dissociation of residual hydrocarbons and water molecules, followed by a chemical reaction between adsorbed carbon and oxygen atoms. © 2012 American Vacuum Society.
[<http://dx.doi.org/10.1116/1.4718426>]

I. INTRODUCTION

Deposition and reaction of carbon on Ru have been the subject of major interest for the past several years,¹ especially in relation to the development of reflective mirrors for the next generation extreme ultraviolet lithography (EUVL) system using 13.5 nm wavelength of light.^{2–4} Recently, extensive research has been carried out on the adsorption,⁵ diffusion,⁵ and/or extreme ultraviolet (EUV)-induced dissociation⁵ of hydrocarbons on a Ru capping layer of Si/Mo multilayer mirrors (MLMs),^{6,7} and the subsequent impact on reflectivity,⁸ which is a function of the Ru layer thickness.⁹ The focus on photochemistry on the Ru surface arises predominantly from the adverse role in extreme ultraviolet reflectivity (EUVR)⁸ of MLMs. Research suggests that the EUV radiation induced surface contamination is associated with: (1) direct photo-dissociation in which the adsorbate on the mirror surface is electronically excited during photo-absorption followed by dissociation into smaller fragments, and (2) indirect dissociation, where the electron-mediated adsorbate decomposition is governed by photoemitted secondary electrons (SEs) from the mirror surface.^{5,10} However, it was reported in a recent theoretical study that EUV-induced C growth is governed by direct excitation induced dissociation rather than SE-mediated decomposition of residual hydrocarbons.⁵ Recent studies showed that a graphitic film, which is harmful for mirror reflectivity, can grow on a Ru single crystal by low energy electron irradiation in the presence of hydrocarbons.^{7,10} Although electrons have been used to simulate the SE irradiation of hydrocarbons under EUV exposure,^{7,10} the effect of SEs on successive mirror reflectivity has not yet been studied so far in detail. In fact, this is a critical issue toward the success of the EUVL technology as this system requires several mirrors for printing nanoscale features.²

X-ray photoelectron spectroscopy (XPS) is commonly used for estimating carbon contamination in mirrors.¹¹ However, Auger electron spectroscopy (AES) is better suited

for analyzing carbon contamination since it is far more sensitive than XPS in determining elements with low atomic numbers (except hydrogen and helium).^{12,13} It should be remembered that similar to XPS signals, there could be overlapping of Auger peaks in multielement samples, as in the Ru/C system.^{14–16} This will affect elemental sensitivity. However, less prominent but isolated peaks can be used for AES analysis in the case of Ru,¹⁷ whereas this technique is very useful for precise analysis of C on target materials such as Rh, Au, etc., where the respective Auger peak position is well separated from C. In addition, by using a primary electron beam energy ≥ 2 keV, one can minimize the carbon deposition process via dissociation of adsorbed hydrocarbons⁷ due to low secondary electron yield (δ).¹⁸ This is also confirmed in the present study. Moreover, because the electron beam can damage the surface composition of a variety of samples, especially for alloys, it is therefore recommended to use a low electron beam flux to minimize damage during AES analysis.¹³ Sequential scans in AES further allow us to follow electron induced damage by looking at the spectral differences with electron exposure.¹³ AES has also been used to study ion beam sputtering induced damage in alloy composition¹⁹ where the Auger signal depends on the geometrical factors (such as surface roughening, shadowing effects, etc.) and preferential sputtering.²⁰

In this article, we report on the experimental protocol to follow electron-induced growth and cleaning of carbonaceous Ru surfaces by AES and EUVR. In particular, we show EUV-induced deposition of carbon on a Ru surface in the presence of additional photoelectrons (PEs) from the focusing Ru mirror of our EUV setup¹⁷ and the formation of a carbide layer with increasing carbon coverage, whereas carbon desorption will be accelerated with electron exposure in sequential AES. In fact, PE-assisted carbon deposition on a Ru surface will be discussed in the framework of EUV-induced dissociation of residual hydrocarbons, and verified further by monitoring the corresponding EUVR. A systematic decrease in reflectivity with increasing EUV exposure in the presence of additional

^{a)}Electronic mail: akanjilal@purdue.edu

PEs from the focusing Ru mirror (called eEUV in the following) has been noticed. Moreover, AES measurements show desorption of oxygen in parallel with carbon growth as a function of eEUV exposure.

II. EXPERIMENT

The experiments were performed at the materials characterization laboratory IMPACT at CMUXE that hosts an ultrahigh vacuum (UHV) chamber equipped with *in situ* diagnostic tools such as XPS, AES, EUVR, etc..^{17,21} To create a chamber condition similar to a EUVL system,⁶ we did not bake the UHV chamber, giving a base pressure of $\sim 1.8 \times 10^{-8}$ Torr. Since the residual gases in the chamber are known to control the growth of carbon and oxidation of the target surface,²² a residual gas analyzer (RGA-100) was used to identify the gaseous components. It reveals a partial pressure of water on the order of $\sim 2.2 \times 10^{-9}$ Torr with respect to nitrogen, as well as different background hydrocarbons such as methane, acetone, ethyl alcohol, methyl alcohol, benzene, toluene, and methane in conjunction with hydrogen. The XPS measurements were performed using an Al- K_{α} radiation source ($h\nu = 1486.65$ eV) where the PEs emitted at 45° from the target surface (giving a sample current of ~ 120 nA) were analyzed by a SPECS Phoibos-100 hemispherical electron analyzer (HEA)¹⁷ with an energy resolution of 0.85 eV. Calibration of the binding energy scale with respect to the measured kinetic energy (KE) was made using silver Fermi edge. A SPECS electron gun (on the x-axis) situated at an angle of 65° from the target surface (without rotating the sample toward HEA along the y-axis) at the center of the UHV chamber¹⁷ was used for AES as well as for sequential AES measurements. Grazing incidence EUVR has been investigated (with the help of a reflecting photodiode at an angle of $\sim 15^{\circ}$)¹⁷ with the help of Phoenix EUV source²³ that emits light in the range of 12.5–15 nm with a peak maximum at ~ 13.5 nm (92 eV), and two calibrated EUV photodiodes from International Radiation Detectors Inc. The estimated EUV total beam power reaching the sample surface is ~ 0.3 μ W, whereas the total power of the photons with wavelength 13.5 nm (within 2% bandwidth) is ~ 0.1 μ W.¹¹ The EUV beam size was as big as the investigating area, while the sample current was changed from -0.6 to 0.5 nA with and without additional PEs from the focusing mirror; see Ref. 17 for details. In fact, the target holder is insulated from the chamber and the sample current was measured from the target in a series with a grounded Keithley-6487 pico-ammeter. The error in the measured reflectivity was found to be about $\pm 4\%$. A 50 nm thick Ru film was grown on a *p*-type Si(100) wafer for our experiments and was diced into pieces with an average area of 1×1 cm². The target surface was sputter cleaned by 2 keV Ar⁺ for 15 min (optimized) with a beam current of ~ 410 nA. The cleanliness of the Ru surface was monitored by AES *in situ* by a 2 keV electron beam, giving a sample current of ~ 430 nA. We should also note here that the electron beam was not scanned during AES and sequential AES measurements, as the spot size of the electron beam was as big as the

area of the target surface. During AES analysis, the electron flux was estimated to be $\sim 5.3 \times 10^{11}$ electrons/cm² s, whereas the electron fluence for each scan was found to be $\sim 1.6 \times 10^{14}$ electrons/cm². As the EUV source is mounted in a separate vacuum chamber with a differential pumping arrangement, the working pressure of the experimental chamber was $\sim 3.1 \times 10^{-8}$ Torr for all our experiments.

III. RESULTS AND DISCUSSION

Figure 1 exhibits a sequence of Auger spectra in the integral mode within 190–290 eV (a) and 500–530 eV (b), and their derivative, $dN(E)/dE$ mode in the range of 190–290 eV (c). The Auger spectra were recorded from a sputter cleaned Ru surface (marked by “0”) and after being exposed to eEUV for 1 min in each step (Fig. 1). The Auger features originating from a sputter cleaned sample in Fig. 1(a) appear as peaks at ~ 201 , 231, and 273 eV on a large background of inelastically scattered electrons, while these features are gradually terminated followed by the change in slope and appearance of a carbide peak at ~ 260 eV (Ref. 14) with increasing eEUV exposure. In addition, a small peak at ~ 514 eV in a sputter cleaned sample [Fig. 1(b)] indicates that the Ru surface is not free of O, while it disappears gradually with eEUV exposure. Differentiating the $N(E)$ spectra in the range of 190–290 eV [Fig. 1(c)], Auger features become prominent relative to the background, and therefore allow to distinguish elements from their KEs. This is also advantageous to track the relative change in peak intensity

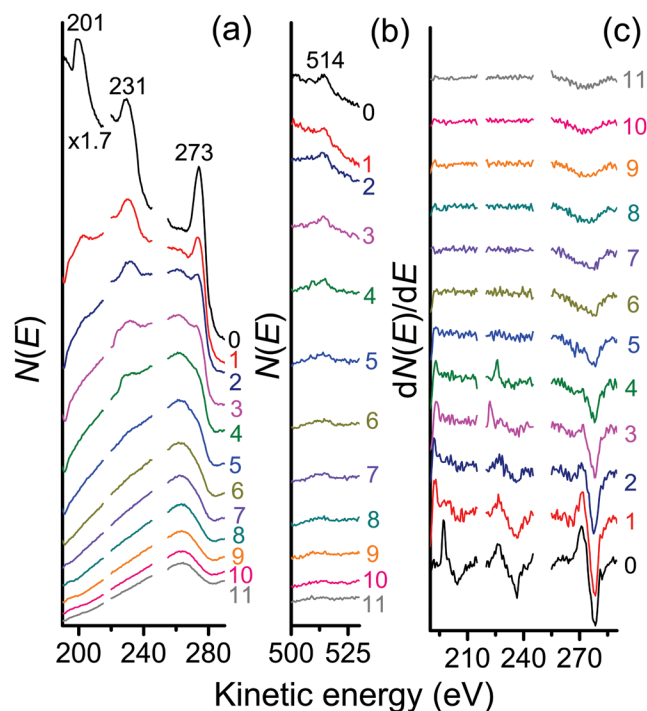


FIG. 1. (Color online) Auger spectra obtained from a Ru surface in the integral, $N(E)$, mode in the KE range of 190–290 eV (a) and 500–530 eV (b), where the derivative, $dN(E)/dE$, mode in the KE range of 190–290 eV is shown in (c). The spectrum recorded after sputter cleaning is marked by 0, while the spectra monitored after being exposed to eEUV for 1 min in each step are indicated by “1”–“11.”

and shape with eEUV exposure. When assigning Auger peaks of sputter cleaned Ru films, we have checked all possible Ru peaks in the range of 200–274 eV.^{12,24} Although the Ru *MNN* peaks situated at ~ 201 and 231 eV are not interfering with different C *KLL* lines¹⁴ (depending on chemical surroundings),²⁵ the strong Ru peak at ~ 274 eV (Ref. 12) overlaps with the C *KLL* transition at ~ 272 eV (Ref. 15) and thus makes the matter complicated. Nevertheless, the eEUV mediated change in a transition profile of the combined Ru and C Auger signal peaking at ~ 273 eV (Fig. 1) supports the growth of carbon in the light of dissociation of adsorbed hydrocarbons on Ru.⁶ Although C atoms were found to be chemisorbed on the Ru surface or accommodated in the form of hydrocarbon fragments (analyzed by XPS), we found the formation of carbide as well using AES.¹⁷ The Auger peak at ~ 514 eV [Fig. 1(b)] indicates oxygen uptake on Ru during Ar^+ sputtering due to the formation of defects at the surface.²⁶

In order to distinguish the effect of additional PEs from the focusing Ru mirror on carbon deposition, we have also carried out AES measurements on Ru by exposing it to EUV only by screening out additional PEs for 1 min in every step (Fig. 2). Although Auger peaks in the $N(E)$ spectra were suppressed in the very beginning of EUV exposure within 190–290 eV [Fig. 2(a)], no significant variation was observed in the O region [Fig. 2(b)]. The first derivative of the $N(E)$ spectra [Fig. 2(c)] also shows a slight change in Auger peaks in the beginning of EUV exposure. These results confirm that the 2 keV primary electrons are suitable for AES studies and do not have a significant effect on the C deposition process by dissociating hydrocarbons.⁷

Since the Ru mirror reflectivity is sensitive to carbon deposition,⁸ we also examined EUVR in every alternating step of AES either by exposing the Ru mirror surface to eEUV or EUV only (Fig. 3). As is apparent, the eEUV-induced decrease in EUVR indicates the increase in carbon coverage, whereas no drastic change in reflectivity was observed when excited with EUV alone, indicating that the 2 keV electron beam did not have much of an effect on carbon deposition during AES measurements (Fig. 2). Based on the above observations, we can therefore conclude that *additional PEs can play a decisive role in depositing carbon on the Ru surface.*

In order to follow the variation in carbon growth, we measured the ratio of the peak-to-peak values of the 273 eV to the 231 eV peaks, where the calculated values for EUV exposed sample (solid circles) are superimposed on the corresponding eEUV values (solid squares) for direct comparison (inset, Fig. 3). Clearly, the carbon growth is much lower with EUV alone than with eEUV. However, the data points for the EUV exposed sample fluctuate within the error bar. The difference in EUV-induced carbon growth with and without PEs can also be correlated to the line shapes of the recorded integral spectra, especially the slope of the background in Figs. 1(a) and 2(a), respectively.

Compared with the EUV exposed sample (Fig. 2), the eEUV-induced gradual deposition of carbon causes the negative signal to grow at 273 eV by suppressing the 231 eV peak in the $dN(E)/dE$ mode [Fig. 1(c)], while the carbide

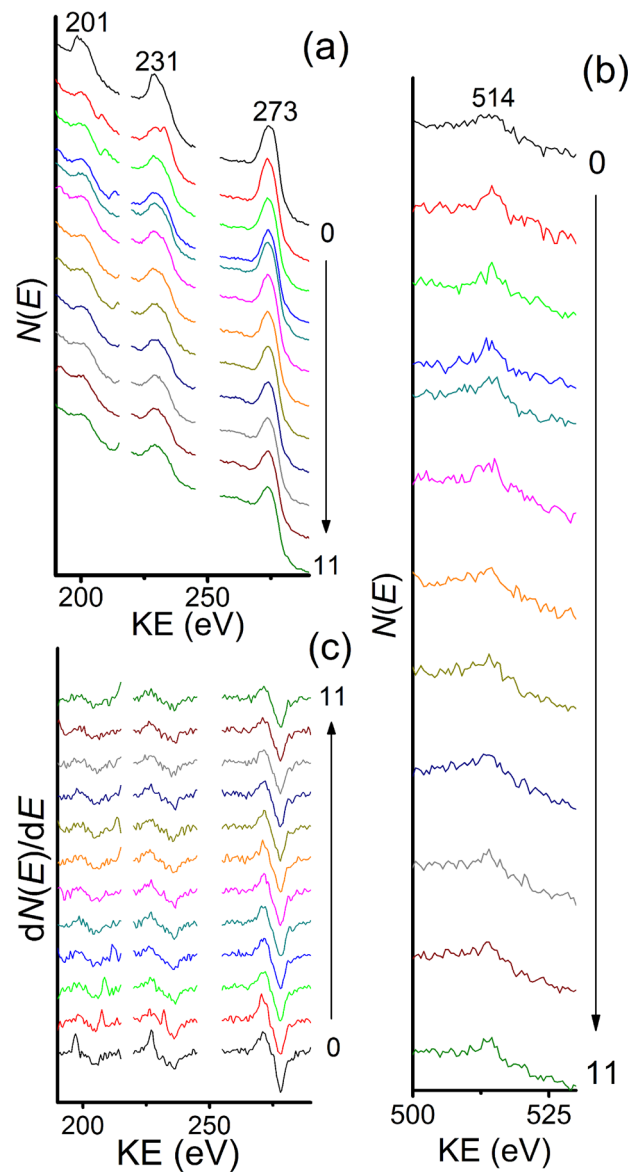


FIG. 2. (Color online) Auger spectra obtained from a Ru surface in the integral, $N(E)$, mode in the KE range of 190–290 eV (a) and 500–530 eV (b), where the derivative, $dN(E)/dE$, mode in the KE range of 190–290 eV is shown in (c). The spectrum recorded after sputter cleaning is marked by 0, while the spectra monitored after being exposed to EUV for 1 min in each step are indicated by 1–11. The spectrum recorded after sputter cleaning is multiplied by 1.7 for clarity.

peak situated at ~ 260 eV (Ref. 14) becomes apparent in the $N(E)$ mode [Fig. 1(a)]. Moreover, the slow disappearance of the O *KLL* peak at ~ 514 eV with eEUV exposure [Fig. 1(b)] can be discussed in light of the PE-induced desorption of O either via the formation of O_2 in an O-rich environment or the creation of surface defects (*i.e.*, oxygen vacancies).⁷ In fact, the formation of oxide species relies on the reaction of a fractional carbon with dissociated fragments of water molecules (mainly free O) on Ru, where the adsorption of water molecules depends on several variables that include binding energy, sticking coefficient, lifetime, chamber pressure, etc.⁶

Since the O peak intensity at ~ 514 eV was found to be almost unaffected during EUV exposure [Fig. 2(b)], we

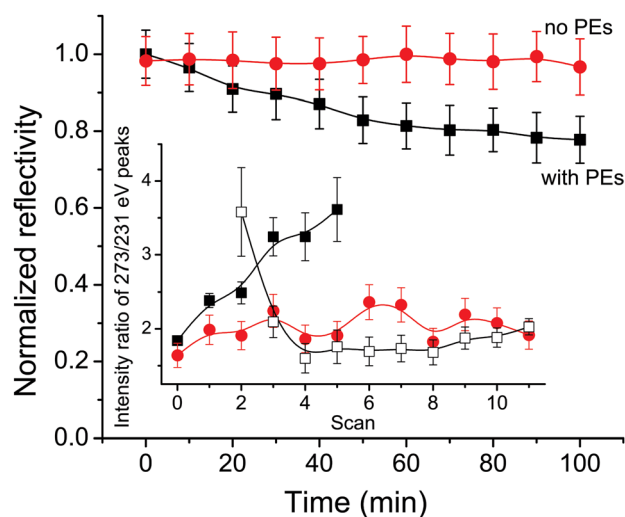


FIG. 3. (Color online) Normalized EUVR of Ru with and without additional PEs, recorded by averaging over 1 min in each step. Inset shows the peak-to-peak intensity ratio of the 273 to 231 eV peaks, derived from differential Auger spectra in the range of 190–290 eV by exposing sputter cleaned Ru (represented by 0 in abscissa) to EUV (solid circles) and eEUV (solid squares) radiation for 1 min in each successive scan, and in sequential AES (open squares) on a carbonaceous Ru surface, prepared by exposing Ru to eEUV radiation for 1 h (represented by 0 in abscissa). The absence of a few points in the plots with solid and open squares is due to the absence of any Ru signal at 231 eV.

believe that *the energetic electron beam alone in AES is neither efficient enough in depositing carbon by decomposing hydrocarbons nor removing oxygen from Ru*. In fact, comparing Figs. 1(b) and 2(b), we can conclude that the kinetics behind O desorption is most likely controlled by C growth rate on Ru. In this way, fluctuation in C deposition under EUV exposure (inset, Fig. 3), and so the insignificant change in EUVR (Fig. 3) can be explained in light of the competition between oxidation and carbonization of the Ru surface via EUV-induced simultaneous decomposition of residual hydrocarbons and water molecules on Ru.^{6,8}

In an attempt to understand the electron-induced sputtering of a carbonaceous Ru surface (prepared by exposing Ru to eEUV for 1 h) in AES, sequential Auger spectra were monitored (Fig. 4). One can see the electron-assisted modification in the $N(E)$ spectra in two different KE regions [see Figs. 4(a) and 4(b)], while the $dN(E)/dE$ results in the KE range of 190–290 eV are displayed in Fig. 4(c). By suppressing the carbide peak at ~ 260 eV,¹⁴ although a slow evolution of the Ru/C peak at ~ 273 eV together with Ru 201 and 231 eV peaks can be observed in the $N(E)$ spectra with electron exposure [Fig. 4(a)], no significant variation in the O KLL peak at ~ 514 eV was found [Fig. 4(b)]. Despite the observation of a clear change in the $N(E)$ line shapes with electron exposure, calculation of the peak-to-peak intensity ratio of the 273 eV to the 231 eV peaks (open squares, inset, Fig. 3) from Fig. 4(c) poses the removal of C atoms from the Ru surface. In fact, the positive going peak at ~ 273 eV with electron exposure [marked by “i” to “xi” in Fig. 4(c)] is the fingerprint of increasing Ru contribution by removing carbon.¹⁶ We should note that the chamber base pressure

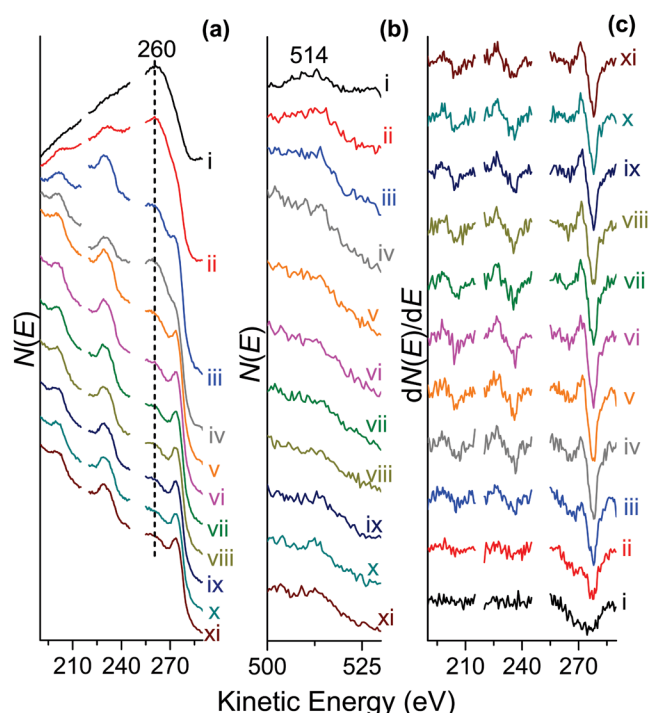


FIG. 4. (Color online) Sequential Auger spectra from a Ru surface in the integral, $N(E)$, mode in the KE range of 190–290 eV (a) and 500–530 eV (b), where the derivative, $dN(E)/dE$, mode in the KE range of 190–290 eV is shown in (c). The spectrum, recorded after contaminating the surface by exposing to eEUV for 1 h, is marked by i, while the Auger spectra monitored in the consecutive scans are indicated by i–xi. The vertical dashed line (a) is given as a guide for the eyes to follow the change in line shape of the carbide phase peaking at 260 eV. The time interval for each step of lines i–xi was 305 s, and the total electron fluence was estimated to be $\sim 1.8 \times 10^{15}$ electrons/cm².

remained similar in each experiment and results were repeatable in different runs.

Now the question arises: why is the electron beam not able to remove O from the Ru surface if it can do so for C? The answer is two-fold: First, the C growth rate is most probably lower than the sputtering rate, while sputtered O can be replaced immediately by the newly created O via SE-enhanced dissociation of water molecules.⁶ Second, the creation of a large number of free O not only accelerates C desorption by forming volatile carbon oxides,⁶ but also can react with the exposed Ru surface²⁶ and thus increase the surface lifetime of O. Since carbon desorption is not a one step process, we will discuss the mechanism involved in detail in the following. Although the water molecules interact weakly with the C coated layer, electron-induced C desorption is able to create a large number of surface defects (O vacancies), which as a result allow free O atoms to interact with underlying Ru atoms.⁷ Although the peak-to-peak values of the 273 eV/231 eV peaks are almost identical after Ar⁺ sputtering and after the fourth scan in sequential AES (inset, Fig. 3), the relatively small upper-half/lower-half ratio of the 273 eV peak in the latter case (0.41) [Fig. 4(c)] with respect to the one after Ar⁺ sputtering (0.56) [Fig. 1(c)] suggest that the electron beam is not efficient enough to sputter out adsorbents from the Ru surface. Hence, we believe that

the second mechanism is playing a pivotal role in controlling C desorption from Ru in sequential AES. In fact, the positive sample current during AES investigation implies that the surface is not flooded with electrons, as opposed to those electrons having energy <270 eV (not shown). This has been investigated separately using an electron gun and will be published elsewhere.²⁷ Based on this observation, the negative target current in the eEUV exposed sample indicates that the low energy PEs from the focusing Ru surface mainly dominate in eEUV experiments.

The above change in surface chemistry can be discussed in detail in terms of δ . Because δ is a function of energy of the injected electrons¹⁸ and photons,⁷ one would expect strong decomposition of hydrocarbons and water molecules on Ru with larger δ , preferably within 100 eV for incident photons,⁷ whereas it is below 1 keV for electrons.¹⁸ This is associated with the difference in photo-ionization cross section and electron-ionization cross section.⁷ In particular, the rate of generation of SEs in the case of electron excitation is a function of depth where the stopping power of the incident electrons plays an important role.¹⁸ The photo-ionization depends primarily on the photon absorption by an atom, followed by electron excitation.²⁸ Because of the difference in ionization processes, the momentum transfer between electrons and lattice (which are responsible in controlling secondary emission)²⁹ cannot, therefore, be identical for the incident photon and electron energies, and so the expected δ . In fact, a photon-stimulated desorption cross section was reported to be smaller than the electron-stimulated desorption cross section on Ru.⁷ This is also due to a larger electron-induced ionization cross section of Ru ($\sim 1 \times 10^{-17}$ cm² for 100 eV electrons) than the photoionization cross section ($\sim 6 \times 10^{-19}$ cm² for 92 eV photons).⁷ Owing to low δ of Ru (~ 0.02 electrons/photon), O removal cross section for 92 eV photons ($\sim 3 \times 10^{-20}$ cm²) was reported to be lower than the one for 100 eV electrons ($\sim 6 \times 10^{-19}$ cm²).⁷ However, we observed an increase in δ with EUV exposure.²¹ Independent of primary electron energy³⁰ and 92 eV photons,⁵ as δ of a typical MLM was found to decrease drastically with increasing carbon coverage, the observed increase in SEs under EUV exposure only²¹ indicates the dominant role of water molecules on Ru for supplying free O atoms,¹¹ which in turn take part in cleaning a fraction of C. A recent observation of a gradual decrease in SEs with eEUV radiation,¹⁷ however, can change the scenario, indicating more hydrocarbons to dissociate than water molecules in the presence of additional PEs that take control of C growth and O desorption (Fig. 1) and so the EUVR (Fig. 3).

Since δ for carbon drops from its maximum (1.06) at ~ 400 eV to 0.37 at 2 keV electrons (see Ref. 18 and references therein), we believe that dissociation efficiency of hydrocarbons and water molecules will be very low on Ru in AES within the present experimental conditions. Moreover, we found a slow C desorption from a carbonaceous Ru surface in the absence of any modification in O peak intensity during sequential AES (Fig. 4). This fact indirectly confirms the dominance of free O over C growth, leading to a chemical reaction to form volatile oxides of carbon.⁶ Clearly, free O

atoms play a key role in cleaning C atoms from Ru as a function of electron exposure, which is in accordance with electron-irradiation enhanced cleaning of surface carbon in O environment at room temperature (RT).³¹

In fact, the formation of CO and RuO₂ has been observed by XPS on a sputter cleaned Ru surface under a similar experimental condition.¹¹ Since CO cannot be dissociated at RT and form CO₂ by reacting with O due to a high activation barrier, it is clear that electrons play the decisive role behind the dissociation and/or desorption of CO. A prior report indicates that electrons below 200 eV are efficient enough to dissociate CO into C and O.³² Since the formation of free O under EUV exposure would be the same in different cases via dissociation of water molecules,¹¹ the observed desorption of O by depositing C on Ru with time (see Fig. 1) in the presence of additional PEs confirms (1) the formation of low energy electrons from the focusing Ru mirror and (2) electron-induced dissociation of CO along with water molecules and subsequent recombination of free O atoms to form O₂ in O-rich environment; whereas adsorbed C on a Ru surface will primarily be transformed into carbides.¹⁷ On the contrary, the carbide peak intensity was suppressed with time without any change in O peak intensity (see Fig. 4). Based on our previous discussion, this phenomenon can also be understood on the ground of electron-induced oxidation of carbides in an O-rich environment,³¹ and the formation of CO. Because of a low δ value for 2 keV electrons, the dissociation probability of CO is likely to be negligible. Since the concentration of C was found to be reduced systematically without much change in O intensity in consecutive AES scans (Fig. 4), looking at the AES spectrum of a sputter cleaned sample we believe that the observed result is related to electron-induced desorption of a fraction of CO from the Ru surface.³³ Partial oxidation of CO can also take place at RT due to the catalyzing behavior of hydrous RuO₂ on a Ru surface, leading to the formation of CO₂.³⁴ As carbon was found to pile up with time in the presence of additional PEs (Fig. 1), we can conclude that the catalytic oxidation³⁴ of CO would be negligible for low energy electrons because of their ability to decompose RuO₂.³⁵

IV. SUMMARY

In summary, we report on electron-induced deposition and desorption of carbon on a Ru surface by AES. We show a systematic growth of carbon on Ru in parallel with oxygen desorption under eEUV exposure using AES and EUVR, where the latter process shows a gradual decrease in EUVR with increasing carbon deposition in time. However, no significant variation in carbon coverage and O desorption was noticed, nor the EUVR when Ru was exposed to EUV radiation without additional PEs. Moreover, sequential AES spectra were recorded from a carbon coated Ru, showing gradual desorption of C without much change in O peak intensity with electron exposure. All these results were discussed on the ground of a competition between EUV and/or electron induced dissociation processes of residual hydrocarbons and water molecules. The present results highlight the crucial

role of SEs in controlling the relative contribution of carbon and free O, and thus their chemical reaction for desorbing C from the Ru surface. We also show the usefulness of AES in tracking C growth without damaging the Ru surface by electron irradiation.

ACKNOWLEDGMENTS

This work was partially supported by SEMATECH Inc. and Purdue University.

- ¹J. Hrbek, *J. Vac. Sci. Technol. A* **4**, 86 (1986).
- ²S. Bajt, N. V. Edwards, and T. E. Madey, *Surf. Sci. Rep.* **63**, 73 (2008).
- ³H. Over, Y. B. He, A. Farkas, G. Mellau, C. Korte, M. Knapp, M. Chandhok, and M. Fang, *J. Vac. Sci. Technol. B* **25**, 1123 (2007).
- ⁴E. Louis, A. E. Yakshin, T. Tsarfati, and F. Bijkerk, *Prog. Surf. Sci.* **86**, 255 (2011).
- ⁵J. Hollenshead and L. Klebanoff, *J. Vac. Sci. Technol. B* **24**, 64 (2006).
- ⁶T. E. Madey, N. S. Faradzhev, B. V. Yakshinskiy, and N. V. Edwards, *Appl. Surf. Sci.* **253**, 1691 (2006).
- ⁷B. V. Yakshinskiy, R. Wasielewski, E. Loginova, M. N. Hedhili, and T. E. Madey, *Surf. Sci.* **602**, 3220 (2008).
- ⁸K. Koida and M. Niibe, *Appl. Surf. Sci.* **256**, 1171 (2009).
- ⁹P. Y. Yan, E. Spiller, and P. Mirkarimi, *J. Vac. Sci. Technol. B* **25**, 1859 (2007).
- ¹⁰G. Kyriakou, D. J. Davis, R. B. Grant, D. J. Watson, A. Keen, M. S. Tikhov, and R. M. Lambert, *J. Phys. Chem. C* **111**, 4491 (2007).
- ¹¹A. Al-Ajlony, A. Kanjilal, M. Catalfano, M. Fields, S. S. Harilal, and A. Hassanein, *J. Vac. Sci. Technol. B* **30**, 021601 (2012).
- ¹²D. Briggs and M.P. Seah, *Practical Surface Analysis by Auger and X-ray Photoelectron Spectroscopy* (John Wiley & Sons Ltd., New York, 1983).
- ¹³J. C. Rivière and S. Myhra, *Handbook of Surface and Interface Analysis* (CRC Press, Taylor & Francis Group, Boca Raton, FL, 2009).
- ¹⁴M. J. Vanstaden and J. P. Roux, *Appl. Surf. Sci.* **44**, 259 (1990).
- ¹⁵R. Pfandzelter, G. Steierl, and C. Rau, *Phys. Rev. Lett.* **74**, 3467 (1995).
- ¹⁶D. W. Goodman and J. M. White, *Surf. Sci.* **90**, 201 (1979).
- ¹⁷A. Kanjilal, M. Catalfano, S. S. Harilal, and A. Hassanein, *J. Appl. Phys.* **111**, 063518 (2012).
- ¹⁸Y. H. Lin and D. C. Joy, *Surf. Interface Anal.* **37**, 895 (2005).
- ¹⁹S. Valeri, R. Tonini, and G. Ottaviani, *Phys. Rev. B* **38**, 13282 (1988).
- ²⁰D. F. Mitchell, G. I. Sproule, and M. J. Graham, *J. Vac. Sci. Technol.* **18**, 690 (1981).
- ²¹M. Catalfano, A. Kanjilal, A. Al-Ajlony, S. S. Harilal, and A. Hassanein, *J. Appl. Phys.* **111**, 016103 (2012).
- ²²S. B. Hill, I. Ermanoski, C. Tarrio, T. B. Lucatorto, T. E. Madey, S. Bajt, M. Fang, and M. Chandhok, *Proc. SPIE* **6517**, 65170G (2007); M. Niibe and K. Koida, *Proc. SPIE* **7361**, 73610L (2009).
- ²³A. Egbert *et al.*, *J. Microlithogr., Microfabr., Microsyst.* **2**, 136 (2003).
- ²⁴L. E. Davis, N. C. MacDonald, P. W. Plamberg, G. E. Riach, and R. E. Weber, *Handbook of Auger Electron Spectroscopy* (Physical Electronics Industries, Inc., Eden Prairie, Minnesota 1976).
- ²⁵B. Lesiak, P. Mrozek, A. Jablonski, and A. Jozwik, *Surf. Interface Anal.* **8**, 121 (1986).
- ²⁶R. Blume, H. Niehus, H. Conrad, and A. Bottcher, *J. Phys. Chem. B* **108**, 14332 (2004).
- ²⁷M. Catalfano, A. Kanjilal, A. Al-Ajlony, S. S. Harilal, and A. Hassanein (to be published).
- ²⁸S. Hufner, *Photoelectron Spectroscopy: Principles and Applications* (Springer-Verlag, Berlin, 1995).
- ²⁹E. M. Baroody, *Phys. Rev.* **78**, 780 (1950).
- ³⁰J. Chen *et al.*, *Appl. Surf. Sci.* **257**, 354 (2010).
- ³¹D. J. Davis, G. Kyriakou, R. B. Grant, M. S. Tikhov, and R. M. Lambert, *J. Phys. Chem. C* **111**, 12165 (2007).
- ³²P. C. Cosby, *J. Chem. Phys.* **98**, 7804 (1993).
- ³³J. C. Fuggle, E. Umbach, P. Feulner, and D. Menzel, *Surf. Sci.* **64**, 69 (1977).
- ³⁴L. Zhang and H. Kisch, *Angew. Chem. Int. Ed.* **39**, 3921 (2000).
- ³⁵A. Al-Ajlony, A. Kanjilal, M. Catalfano, S. S. Harilal, A. Hassanein, and B. Rice, *Proc. SPIE* **8322**, 832232 (2012).